



Empirical Checking of Ferromagnetic Resonance of a Solution with Magnetosomes in the 2.40-2.55 GHz Range

Delia Bianca Deaconescu¹, Paula Pavaluca², David Vatamanu^{2,3}, Cristina Moiescu⁴, Lucian Barbu-Tudoran⁵ and Simona Miclaus*³

¹Doctoral School of Electrical Engineering, Technical University of Cluj-Napoca, Cluj, Romania

²Engineering Faculty, "Lucian Blaga" University, Sibiu, Romania

³Communication and IT Department, "Nicolae Balcescu" Land Forces Academy, Sibiu, Romania

⁴Department of Microbiology, Institute of Biology Bucharest, Romanian Academy, Bucharest, Romania

⁵Department of Molecular Biology & Biotechnology, Babes-Bolyai University, Cluj-Napoca, Romania

*simo.miclaus@gmail.com (corresponding author)

ABSTRACT

Magnetosomes extracted from *Magnetospirillum gryphiswaldense* bacteria were suspended in a water-based solution and their ferromagnetic resonance effect have been traced by experimental means. A set-up providing incident electric field strengths of 1100-1200 V/m was used to expose the non-magnetic and magnetic liquid samples to continuous wave at four frequencies in the range (2.40-2.55) GHz. The magnetic sample with a weight concentration of 10^3 g/l of magnetite showed a clear resonance at high power exposure, when exposed in the microwave oven for 10 seconds. In the laboratory controlled field exposure but at much lower field strength, only the 2.55 GHz frequency stimulus induced a small resonance. After 15 minutes of exposure, the slope of the heating rate of magnetosome solution was 2.4 times larger than that of the similar but non-magnetic liquid.

Key words: magnetosome, specific power loss, microwaves hyperthermia, magnetite nanoparticle

INTRODUCTION

Magnetosomes are naturally synthesized magnetite (Fe_3O_4) nanoparticles enveloped in a biological membrane and chained in a form of flattened helical chains inside magnetotactic bacteria cells. Their main role is to sustain magnetic field orientation during movement of bacteria. However, a number of very interesting applications exist based on the fact that such high purity magnetite nanoparticles may be used in various applications of medicine and biotechnology [1]. One of the applications is magnetic hyperthermia, which classically use intense electromagnetic fields (EMF) at low frequency range, (50-450) kHz, to heat up magnetite nanoparticles. When injected in specific locations of tissues, such nanoparticles may destroy, by heating, for example cancer cells, when the target volume is exposed to EMF. The magnetic hyperthermia at low frequencies is well represented in the literature by numerous and continuous findings [2], [3]. However, magnetic hyperthermia at ultra-high frequencies has been much less explored, mainly because the costs of producing intense EMF at such frequencies is very expensive and because the penetration depth in tissues, at higher frequencies, decreases very much. With the development of wireless communication technologies, even if the emitted powers are not large for such devices, a question may raise about the contribution to the total heating of tissues, due to the presence of magnetite nanoparticles in some body parts/tissues and exposure of those parts to very/ultra-high frequency fields emitted by telecommunication sources [4-5].

A major contribution to the knowledge of the response of magnetic nanoparticle fluids to ultra-high frequency fields exposure, including microwaves, has been brought by the research group of Fannin [6-9], which showed that different resonances of EMF absorption are observable in the 1-3 GHz range at different type and dimensions of magnetic nanoparticles, including peculiarities such as geometric and magnetic anisotropy. The phenomenon behind resonant behaviour is the ferromagnetic resonance (FMR), which practically quantify the coupling between the EMF and the magnetization of the traversed medium [10-13]. This coupling phenomena induces the loss of the incident's wave power

while the absorption is due to the precessing of the magnetization vector of the material (Larmor precession). The lost materializes into dissipated heat. The coupling occurs when the frequency f of the incident wave equals the Larmor frequency of the substance and when the polarization of the wave matches the orientation of the magnetization vector of the material.

In 1998, experimental measurements of the resonant properties of magnetic fluids in the low-GHz frequency range proved that the complex magnetic permeability/complex susceptibility of ferrofluids, including the ones based on Fe_3O_4 nanoparticles, were frequency dependent [6]. The resonant frequency and the real part of the susceptibility varied with the magnetic nanoparticles' concentration and with their magnetic anisotropy, while the imaginary susceptibility presented peaks at specific frequencies. Therefore, heating peaks are expected for liquid suspensions containing magnetite nanoparticles which were not much explored in this frequency range [14-16]. The metrics of the magnetic hyperthermia refers in the literature at either the specific power loss (SPL) or the specific absorption rate (SAR) of energy dissipation, both expressed in W/kg. There is an immediate relationship between this measure and the temperature increase, ΔT :

$$SPL = c * \Delta T \quad (1)$$

where c is the specific heat of the EMF exposed material.

In the last years, biogenic magnetite nanoparticles present in magnetosomes became a great competitor of their chemically synthesized counterparts, due to their perfect crystallization, larger sizes, and/or chain arrangement, especially in hyperthermia applications [3] where an increased efficiency of hyperthermia was revealed due to the presence of chain-arrangement of magnetosomes compared to the case when they were individually dispersed in the sample, as it happens with all synthetic magnetic nanoparticles [17-20].

Some previous studies of ours indicated that certain small resonances of different liquid suspensions of magnetosomes exist in the low-GHz frequency range [21-22], therefore the present empirical approach aimed at checking the amplitude of the FMR response of a water-based suspension of magnetosomes extracted from *Magnetospirillum gryphiswaldense* bacteria, noted hereafter as MAG, when exposed to microwaves (MW) in the frequency range between (2.40 – 2.55) GHz at incident electric (E) field strengths of the order of 1100-1200 V/m.

DESIGN, MATERIAL, PROCEDURE, TECHNIQUE OR METHODS

The MAG sample was prepared and then characterized by transmission electron microscopy. *Magnetospirillum gryphiswaldense* (DSM-6361) magnetotactic bacteria were grown under microaerobic conditions in a flask standard medium in the laboratory. After reaching the stationary growth phase, the cells were harvested by centrifugation and followed a chemo-physical extraction method of magnetosome chains, as described in [21] and [22]. A field-emission-gun scanning transmission electron microscope (STEM), 80-200 kV, with secondary electron imaging capability, model Hitachi HD2700, allowed imaging of the sample (Fig. 1). It revealed the presence of some of the bacteria cells (partially destroyed) and of the inner magnetosome chains. Post-processing, the dimensional histogram of magnetite nanocrystals in the magnetosomes indicated that magnetite nanoparticles had the dimensions of (39.93 ± 9.23) nm with the median value of 40.73 nm. Fig. 1 contains an enlarged image of a chain to clearly observe not only the black crystals of Fe_3O_4 but also the membranes enveloping each nanoparticle to form the magnetosome and then the whole chains (sustained by a cytoskeleton). The MAG sample contained also water as re-suspension medium, so that the magnetite concentration by weight in the liquid (bacteria cells+water) was measured to be 10^3 g/l. In the experiments, a volume of 0.6 ml of MAG and the same volume of deionized water (noted hereafter WAT), were the samples used for comparison of the temperature increase differences due to EMF exposure. Fig. 1 shows also a larger volume of MAG sample prepared for the experiments (repeated).

The EMF exposure set-up (Fig. 2) was composed of a radiofrequency signal generator model SM 300 from Rohde & Schwarz, a radiofrequency amplifier up to 13 W model Ophir 5050, a horn antenna BBHA 9120A from Schwarzbeck, a fiber optic temperature sensor with instrument model Optocon OEM from Weidmann and an isotropic E-field probe model EM Sense 10 connected with a fiber optic cable to the EM Center, from ETS Lindgren. The interest frequencies at which the samples were exposed were: 2.4 GHz, 2.45 GHz, 2.5 GHz and 2.55 GHz. The maximum power delivered to the antenna was 13 W, but taking into account its directional gain and its total efficiency, which were dependent on the frequency, slightly different E-field strengths were obtained in the same location. Therefore, the sample were always positioned after the E-field level measurement, so as to always preserve its value at incidence to the sample.

The functioning and data recordings of the fiber optic temperature sensor was driven by Fotemp Assistant 2 software. The temperature was recorded every 2 seconds as an average over the sampling frequency of 2 Hz. The total E-field strength was measured by the Probe View V software, which integrates the field strengths from all three orthogonal directions to provide an isotropic response. Since the "background" field level has never exceeded 2 V/m (the system is wide-banded), we considered that the measured values of E, exceeding 1000 V/m, could be estimated with sufficient precision with a wide-band instrument in this case. The exposure system was placed and used in a laboratory, without other shieldings or anechoic measures.

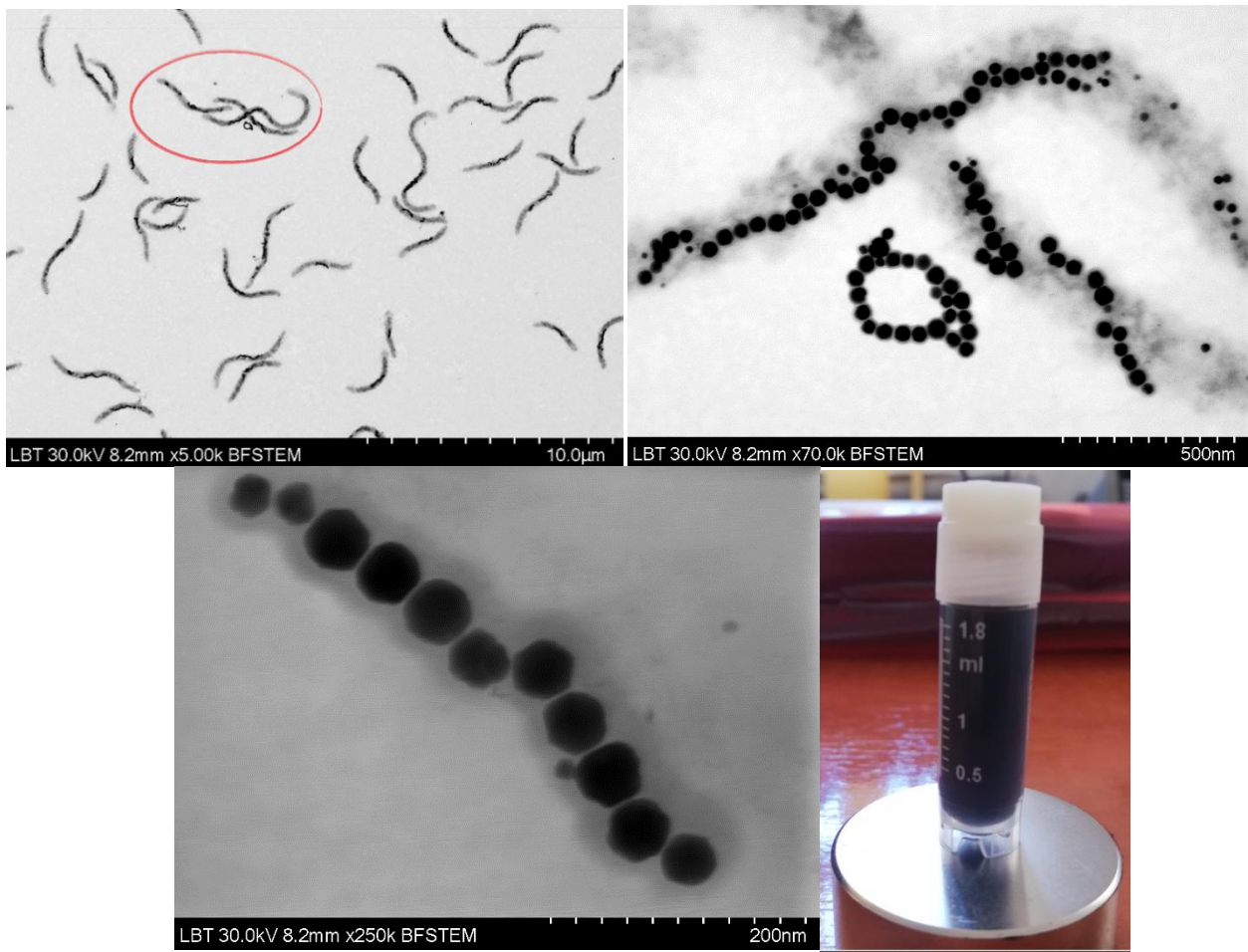


Fig. 1 The TEM Image of the Sample: Bacteria Cells Suspension; Enlarged Inner Chains of Magnetosomes; a Detail of a Chain to See the Magnetite Nanocrystals Enveloped in a Membrane; a photo of the sample of MAG as seen by necked eye

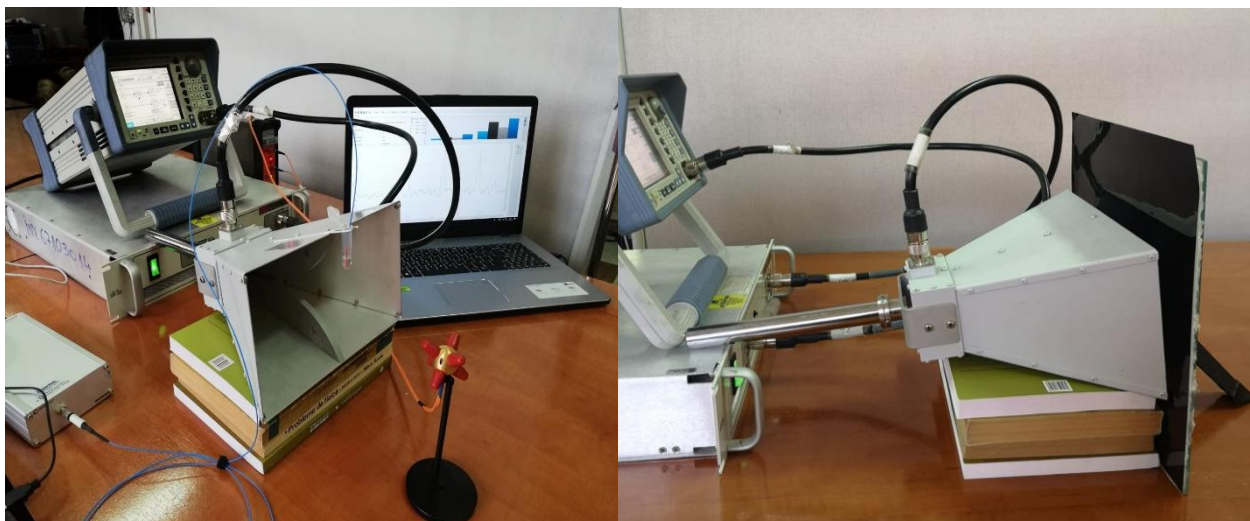


Fig. 2 The measurement set-up showing the horn antenna, the position of the small liquid sample just in front of it (near field exposure condition) and the immersed thin fiber optic temperature probe; in the right side the black sheet is the one containing liquid crystals used to transform the incident field distribution into a thermal image
The E-field strength surface distribution in a vertical plane in front of the horn antenna, where the MAG and WAT probes were then placed sequentially, was obtained by indirect heating image produced in a liquid crystal sheet on plastic film (stock no. 72-375, temperature range 20-25 deg C, produced by Edmund Optics). The thermic image of the

field distribution was obtained in the width of a paper's sheet impregnated by distilled water, with the scope to place the probes where the highest field was obtained in near field conditions, at each inspected frequency.

The same liquid crystal sheet was also used in another exposure system, respectively in a microwave oven. The microwave oven was used as a kind of "reference" to observe, in a first instance, if the MAG sample heats higher than the WAT sample, after a certain amount of time, namely 10 s, at the same incident field strength. The initial heating experiment in the oven was made taking into consideration the field distribution in a multimode resonance cavity [23], [24]. In order to provide the same incident E-field level on both samples, they were placed practically one near the other and the heating image on the liquid crystal sheet should look properly to indicate the same temperature over the whole surface the samples were occupying during irradiation.

RESULTS AND DISCUSSION

In the first experiment we used a microwave oven with a nominal power of 700W in order to observe the final temperature differences that might appear between the two samples, after they were exposed to the same field strength during the same period of time. The magnetron of the microwave oven theoretically emits at 2.45 GHz, but practically there isn't a pure spectral line at this frequency solely, but the emitted frequencies covers a band between (2.43-2.47) GHz, as seen in Fig. 3 – left side. The spectrum from Fig. 3 was captured by using a small E-field probe connected to a swept spectrum analyser set with the max-hold trace type, and the probe was kept a few cm outside the oven's door (leakage field was sensed). In Fig. 3 – right side, it is observed the temperature distribution on the liquid crystal sheet situated in perfect superficial contact with the water-impregnated porous paper, during exposure of the samples in the microwave oven. After 10 s of simultaneous exposure in the same conditions, while almost identical temperature distribution in the plane of exposure is observed, the sample temperatures were different. Fig. 4 shows the temperature differences in the samples, 1.1°C, which maintained during all seven repetitions of the experiment. This finding indicates that a resonant frequency of the MAG sample would be situated in this frequency range.

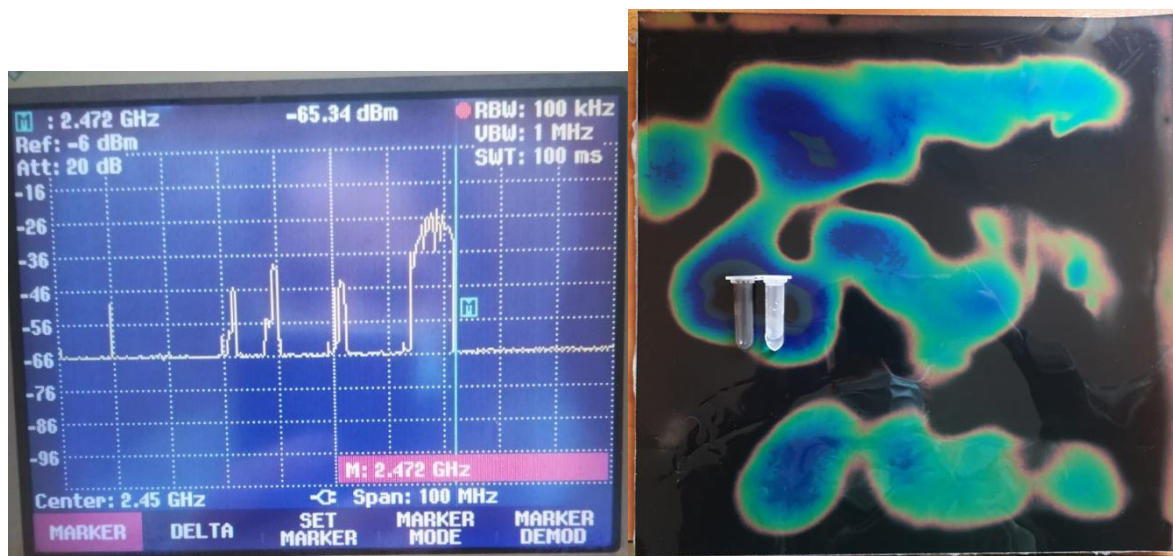


Fig. 3 The spectrum captured from outside of the microwave oven (leakage field) – left side; E-field strength distribution on the surface where the MAG and WAT samples were exposed simultaneously, in the oven

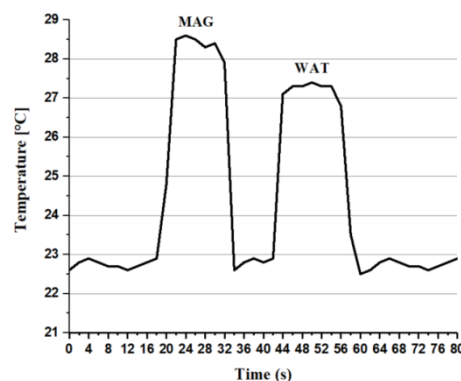


Fig. 4 Temperature differences measured between the samples exposed to the same field strength in the microwave oven post-exposure, after 10 s of continuous exposure

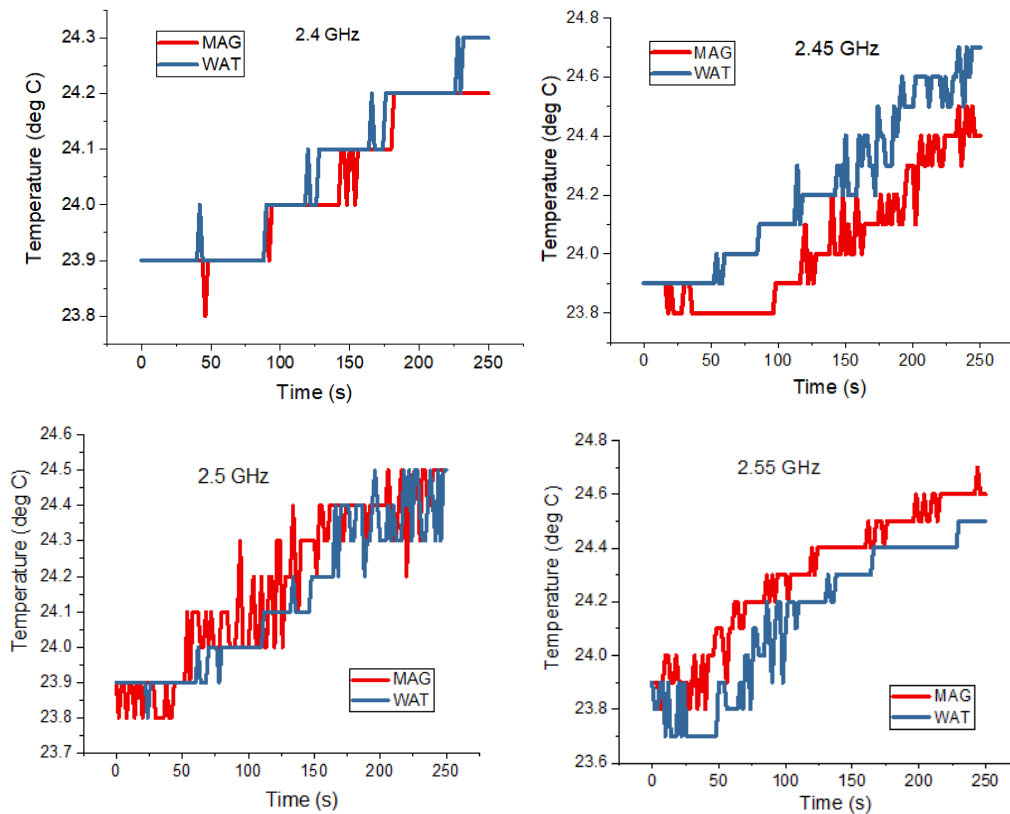


Fig. 5 Heating curves of the magnetic and non-magnetic samples at different frequencies and at E-field strengths of (1100-1200) V/m

The second group of experiments emphasized the rates of temperature increase in time, during controlled (but lower) exposure, comparatively between the MAG and WAT samples, for the four tested frequencies. Fig. 5 refers to all four tested frequencies. A number of five repetitions were enabled at each frequency. The environmental temperature control could not be ensured at a lower value than 0.5 °C variation value. This is the main factor contributing to the uncertainty budget. As observed in Fig. 5, when the samples were exposed at the same E-field strength component, between 1100-1200 V/m, the slope of the heating curves during 260 s of exposure was practically the same for MAG and WAT. This means that MAG doesn't present any resonance at these frequencies.

A third group of experiments proposed following the temperature curves evolution on longer exposure times, namely over 900 s. Repeated results showed that at 2.55 GHz, MAG sample tends to heat up faster than WAT (Fig. 6), indicating that this frequency might represent a resonance of the magnetosome liquid. Extracting 300 s from the heating curves and fitting a linear trend, the slope of temperature increase was 2.4 times larger for MAG than for WAT. Practically, MAG sample heated at a rate of $1.48 \times 10^{-3} \text{ }^\circ\text{C/s}$ while WAT sample heated at a rate of $0.63 \times 10^{-3} \text{ }^\circ\text{C/s}$. This difference corresponds to an incident E-field strength of 1100 V/m. The exposure was made however in the near field of the horn antenna, and the magnetic (H) – field component has not been measured.

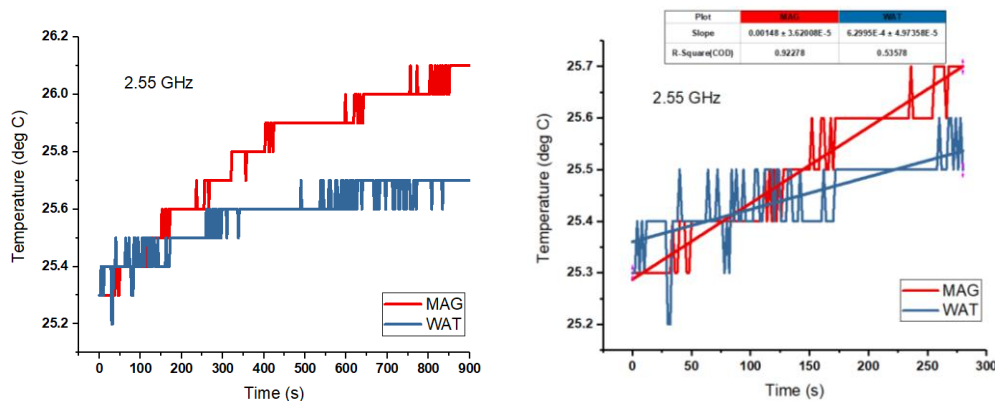


Fig. 6 Heating curves of the samples at 2.55GHz over 15 minutes of exposure with linear fitting over 300 s



Fig. 7 Thermal image of the near field distribution in front of the horn antenna at 2.55 GHz, as a preparation for the exposure location of the samples

The placement location of the samples was chosen based on the thermal image obtained with the liquid crystal film. Fig. 7 shows the thermal print of the field distribution (yet the temperature in the water sheet) in front of the antenna, at 2.55 GHz. The placement of the sheet is shown in Fig. 2 – right side. The samples were placed during exposure in the green zone.

CONCLUSION

Identifying resonance frequencies of liquids containing biogenic magnetite nanoparticles in the ultra-high frequency range was the aim of the present work. Exposure of samples containing magnetosomes in form of chains, each magnetosome containing a magnetite nanocrystal of an average dimension of 40 nm, was applied at four frequencies in the microwave oven's range of frequencies. After 10 s of exposure in the oven, a liquid sample containing magnetosomes with a concentration of 1000 g/l magnetite heated more than the similar liquid sample that didn't contain magnetite. Based on this empirical finding, a set of tests at much lower field strengths (not larger than 1200 V/m) were made, with the objective of quantification the temperature increase differences due to the presence of magnetite in the liquid. Because of the insufficient control of the environmental temperature, and because of very small heating slopes at this field level, clear results could not be obtained. However, at longer exposures, of at least 15 minutes, the magnetosome sample showed larger heating slope than the non-magnetic liquid, at 2.55 GHz. Better controlled experiments are under preparation, because at these frequencies and at the nanometre dimensions of the ferrimagnetic crystals, simulation of heating phenomena due to EMF exposure is not possible.

REFERENCES

- [1]. L Yan, H Da, S Zhang, VM López, and W Wang, Bacterial magnetosome and its potential application, *Microbiological Research*, 2017, 203, 19-28.
- [2]. E Alphanbéry, I Chebbi, F Guyot and M Durand-Dubief, Use of bacterial magnetosomes in the magnetic hyperthermia treatment of tumours: A review, *International Journal of Hyperthermia*, 2013, 29 (8), 801-809.
- [3]. D Gandia, L Gandarias, I Rodrigo, J Robles-García, et al., Unlocking the Potential of Magnetotactic Bacteria as Magnetic Hyperthermia Agents, *Small*, 2019, 15 (41).
- [4]. S Miclaus, M Racuciu, and P Bechet, H-field contribution to the electromagnetic energy deposition in tissues similar to the brain but containing ferrimagnetic particles, during use of face-held radio transceivers, *Progress In Electromagnetics Research B*, 2017, 73, 49-60.
- [5]. S Miclaus, C Iftode, A Miclaus, Would the human brain be able to erect specific effects due to the magnetic field component of an UHF field via magnetite nanoparticles?, *Progress in Electromagnetic Research M*, 2018, 69, 23-36.
- [6]. PC Fannin, Wideband Measurement and Analysis Techniques for the Determination of the Frequency-Dependent, Complex Susceptibility of Magnetic Fluids, *Advances in Chemical Physics*, 1998, 104, 181-292.
- [7]. PC Fannin, CN Marin, I Malaescu, N Stefu, An investigation of the microscopic and macroscopic properties of magnetic fluids, *Physica B: Condensed Matter*, 2007, 388 (1-2), 87-92.
- [8]. I Malaescu, PC Fannin, CN Marin, DLazic, The concept of ferrofluid preheating in the treatment of cancer by magnetic hyperthermia of tissues, *Medical Hypotheses*, 2018, 110, 76-79.

- [9]. PC Fannin, I Malaescu, CN Marin, N Stefu, Frequency and field dependence of the electromagnetic field propagation constant in magnetic fluids in microwave range, *Physics Conference Tim-07*, Timisoara, 2007.
- [10]. DS Schmool, M Schmalzl, Ferromagnetic resonance in magnetic nanoparticle assemblies, *Journal of Non-Crystalline Solids*, 2007, 353, 738-742.
- [11]. LG Abraçado, E Wajnberg, D Motta, CNKeim, K Silva, ET Moreira, U Lins, M Farina, Ferromagnetic resonance of intact cells and isolated crystals from cultured and uncultured magnetite-producing magnetotactic bacteria, *Physical Biology*, 2014, 11 (3).
- [12]. S Ghaisari, M Winklhofer, P Strauch, S Klumpp, D Faivre, Magnetosome Organization in Magnetotactic Bacteria Unraveled by Ferromagnetic Resonance Spectroscopy, *Biophysical Journal*, 2017, 113 (3), 637-644.
- [13]. A Chanda and R Mahendiran, Microwave magnetoimpedance and ferromagnetic resonance in Pr_{0.6}Sr_{0.4}MnO₃, *RSC Advances*, 2019, 9, 29246-29254.
- [14]. K Kim, T Seo, K Sim and Y Kwon, Magnetic Nanoparticle-Assisted Microwave Hyperthermia using an Active Integrated Heat Applicator, *IEEE Transactions on Microwave Theory and Techniques*, 2016, 64 (7), 2184-2197.
- [15]. UrdanetaMaryory, *Enhanced microwave hyperthermia using nanoparticles*, University of Central Florida, USA, 2015.
- [16]. D Walton, H Böhnelt, D Dunlop, Response of magnetic nanoparticles to microwaves, *Applied Physics Letters*, 2004, 85, 5367-5369.
- [17]. D Serantes, K Simeonidis, M Angelakeris, O Chubykalo-Fesenko, et al., Multiplying Magnetic Hyperthermia Response by Nanoparticle Assembling, *The Journal of Physical Chemistry C*, 2014, 118 (11), 5927-5934.
- [18]. E Alphantery, Y Ding, AT Ngo, ZL Wang, LF Wu and MP Pileni, Assemblies of aligned magnetotactic bacteria and extracted magnetosomes: What is the main factor responsible for the magnetic anisotropy?, *ACS Nano*, 2009, 3 (6), 1539-1547.
- [19]. B McWilliams, H Wang, V Binns, S Curto, S Bossmann, P Prakash, Experimental Investigation of Magnetic Nanoparticle-Enhanced Microwave Hyperthermia, *Journal of Functional Biomaterials*, 2017, 8 (3), 21.
- [20]. E Myrovali, N Maniotis, A Makridis, et al., Arrangement at the nanoscale: Effect on magnetic particle hyperthermia, *Scientific Reports*, 2016, 6.
- [21]. S Miclaus, G Mihai, C Moisescu, P Bechet, II Ardelean, L Barbu-Tudoran, S Oancea, M Racuciu, TM Radu, Radiofrequency Stimuli Applied to Suspensions Containing Biogenic Magnetite Nanocrystals: Absorbed Energy Conversion, *2018 International Conference and Exposition on Electrical and Power Engineering (EPE)*, Iasi, Romania, 2018, 0143 – 0148.
- [22]. S Miclaus, G Mihai, P Bechet, II Ardelean, J Karpowicz, C Moisescu, The thermic response of biogenic magnetite suspensions to frequencies in the (0.1-2.9) GHz range, *2018 EMF-Med 1st World Conference on Biomedical Applications of Electromagnetic Fields (EMF-Med)*, Split, Croatia, 2018.
- [23]. T Santos, LC Costa, M Valente, J Monteiro, J Sousa, 3D electromagnetic field simulation in microwave ovens: a tool to control thermal runaway, *Proceedings of the COMSOL Conference*, Paris, France, 2010.
- [24]. D Luan, Y Wang, J Tang, D Jain, Frequency Distribution in Domestic Microwave Ovens and Its Influence on Heating Pattern, *Journal of Food Science*, 2017, 82, 429-436.